Fabrication of cobalt phthalocyanine-TiO_2 with enhanced photocatalytic activity for the removal of MB dye

YUAN CAI[a,b*], LIXIN TANG[a], YUNTAO WANG[a*], NING XU[a], YULONG LI[a], GUOWEI JI[a]
[a]*Jiangsu Research and Development Center of Chemical Engineering Applying Technology, Department of Chemical Engineering, Nanjing Polytechnic Institute, Nanjing 210048, P.R. China*
[b]*College of Chemistry and Chemical Engineering and State Key Laboratory of Materials-Oriented Chemical Engineering, Nanjing Tech University, Nanjing 210009, P.R. China*

Cobalt phthalocyanine dye (CoPc) sensitized TiO_2 composites (CoPc/TiO_2) with visible-light responses were synthesized employing ultrasonic immersing-hydrothermal sensitization method facilely. Scanning electron microscopy (SEM) and transmission electron miscroscopy (TEM) were employed to visually observe the surface morphologies of the samples. We studied the visible-light response using UV-vis diffuse reflectance spectroscopy and optical band gap calculations using the Tauc plot equation. The photocatalytic activities of the as-prepared CoPc/TiO_2 composites were assessed in terms of the degradation rate of methylene blue (MB) solution under visible-light irradiation. The CoPc/TiO_2 (1:3 mass ratio) composites achieved best enhancement of photocatalytic activity. When CoPc/TiO_2 nanocomposites were applied for different photocatalytic degradation cycling times, the degradation rate of MB still reaches 74% which reflects the fact that CoPc/TiO_2 composites have a high photostability in the photocatalytic process. When taking the decomposition rate and photoresponse into consideration, the possible connection action between CoPc and TiO_2 and visible-light induced photocatalytic mechanism of contaminants degradation in the presence of CoPc/TiO_2 nanoparticles were proposed. Potential bonding interaction between CoPc dye and TiO_2 framework improves photogenerated electron-hole pair separation and facilitates photogenerated charge transfer, which gives access to the occurrence of degradation of hazardous materials.

(Received April 7, 2015; accepted June 24, 2015)

Keywords: Cobalt phthalocyanine dye, Titanium dioxide, Band gap calculation, MB degradation

1. Introduction

As is known to all, titanium dioxide (TiO_2) photocatalysts get widely attention in the field of environmental protection due to their thermodynamic stability, non-toxicity, environmental friendly, low cost and high photocatalytic activity without secondary pollution [1-3]. However, the wide band gap of TiO_2 (E_g) up to 3.2 eV greatly limits the sunlight harvesting for various photo-induced reaction, among which the UV light only accounts for just 3-5% of the solar light. An efficient approach to improve the photocatalytic efficiency of TiO_2 in visible-light region and help the separation of charge carriers [4] is fabricating composite photocatalysts by means of noble metal doping, nonmetal doping, semiconductor heterojunction construction and selecting some supporters with excellent electronic transmission capacity such as graphene and carbon nanotube (CNT) [5-13]. The modification method of the organic dye photosensitization has proved to be an efficient method to modify TiO_2 via extending the absorption spectra to visible region for which the organic dye could easier excite by absorbing visible light and faster charge transfer is established between the dye molecular and the semiconductor.

Phthalocyanine dye is one of the most promising sensitizer due to its highly conjugated 18 π electronic system and strong electronic interaction between the big ring system with strong absorption of visible light around 600-700 nm and strong transition in the visible region. Several special structures such as benzene rings and the center of the large ring located on phthalocyanine dye can be modified further which lead to great changes in many properties of different complexes [14-16]. Combined with metal elements, great catalytic performance of the metal phthalocyanine compounds (cobalt phthalocyanine dye (CoPc)) can be explored due to the conjugacy of its macrocyclic ligands, which makes the catalytic reactions occur in the axial plane position easier. The metal phthalocyanine compounds with different levels can be obtained which is conducive to the improvement of the photoelectric conversion efficiency and adjustability of the molecular structure [17]. The band gap of CoPc approached to 2.0 V with strong transition capacity make this non-toxic and inexpensive catalyst a promising category under visible-light illumination [18-21]. As

proposed, the combination of CoPc and TiO_2 plays a fundamental role in determining carrier transport process and sewage dealing capacity. As a widely used dye reagent, MB has much potentially environmental harmfulness because of its high stability which was generally oxidized to harmless carbonate compounds by the photogenerated holes from excited as-prepared CoPc/TiO_2 nanocomposites under illumination.

In present study, cobalt phthalocyanine dye (CoPc) sensitized TiO_2 (CoPc/TiO_2) nanocomposite photocatalysts have been fabricated successfully. Various characterizations such as morphology observations (SEM and TEM), crystalline structure validation (XRD), functional group (FT-IR) and calculation of the optical band-gaps (UV-DRS) were employed to validate the existence of the product. In addition, the photocatalytic activity of CoPc/TiO_2 nanocomposites was evaluated by measuring photodegradation rate of methylene blue (MB) under visible-light irradiation. The photostability of the prepared catalysts was tested, resulting in that relatively high degradation rate could be achieved after 5 cycle experiments. In this decomposition process, MB was mineralized to harmless carbonate compounds. Excellent degradation effect in the present of MB was proposed and visible light-induced photocatalytic mechanism was carried out to be further discussed.

2. Experimental

2.1. Preparation of phthalocyanine dye sensitized TiO_2 nanoparticles

The CoPc dye applied as the photosensitizer was synthesized by a procedure according to reference [22]. The structural formula of CoPc dye is presented in Fig. 1f.

TiO_2 nanoparticles were prepared by using a surfactant-assisted sol-gel method. 34 mL of tetra-n-butyl titanate and 136 mL of absolute ethyl alcohol were stirred to form the A solution. The B solution containing 34 mL of deionized water and isometric absolute ethyl alcohol was mixed with pH around 3-4 adjusted by adding 6.8 mL of nitric acid dropwised. Then the A solution was added into the obtained B solution slowly with a mechanical stirrer until a uniform solution was formed. 0.3 g of sodium dodecyl sulfate (SDS) was added into the above sol solution under continuously stirring. The mixture was stirred for 2 h at room temperature, and then kept 40 mL of as-prepared TiO_2 sol precursor into a three necked flask with reflux condensing tube. 6 mL of phenol and 15 mL of n-heptane were added into the above solution rapidly, 10 mL of formaldehyde solution and 15 mL of n-heptane were added subsequently. The mixture was kept stirring at 90 ^oC until the color of the solution changed to black, then cooled to room temperature followed with a series of post-processing operations. The final gel titanium hydroxide precursor were kept static for 24 h in a vacuum oven at 80 ^oC, calcined at 500 ^oC in air for 3 h to yield TiO_2 nanoparticles.

The CoPc/TiO_2 was prepared via ultrasonic immersing-hydrothermal sensitization method according to the following steps: first, 50 mg of CoPc was dissolved in 250 mL of ethanol under stirring for 30 min to form a uniform solution. Then, 150 mg of TiO_2 nanoparticles were dispersed into this ethanol solution of CoPc. After continuously ultrasonicated for 5 h to form the hybrid solution, then the solution was transferred into a 250 mL Teflon-lined stainless autoclave. The autoclave was kept at 100 °C for 12 h. After cooled to ambient temperature naturally, the precipitate was filtered, washed with slight deionized water and ethanol repeatedly, finally the obtained product was dried at 60 ^oC under vacuum till the constant mass was reached. Then CoPc/TiO_2 nanocomposites were obtained.

2.2. Characterization

Morphologies of the samples were observed on a JEM-2100 transmission electron microscope (TEM) and a Hitachi S4800 scanning electron microscopy (SEM). X-ray diffraction patterns were recorded on a SmartLab-9 (RigaKu Corporation, Japan) automated power X-ray diffraction meter operating at 100 mA and 40 kV using Cu Kα (λ = 0.1541 nm) radiation. The data of 2θ from 20 to 80^o were collected with a step scan of 0.02^o. FT-IR spectra were collected on a Nicolet-6700 spectrometer from Thermo Electron with a resolution of 5 cm^{-1} using anhydrous KBr (Nicolet, United States) as dispersing agent. UV-vis diffuse reflectance spectroscopy (DRS) spectra of the photocatalysts were measured by a UV-vis scanning spectrophotometer (Shimadzu UV-2700) using an integrating sphere and $BaSO_4$ as white standard.

2.3. Photocatalytic activity

The photocatalytic activity of different samples were evaluated by photodegradation of the methylene blue (MB, 25 mg/l) using a 500 W iodine tungsten lamp (Philips, China) with a 400 nm cutoff filter to eliminate the UV light. The reaction suspension was prepared by adding 10 mg of photocatalyst powders into a glass vessel with a circulating water jacket containing 50 mL of the target contaminant aqueous solution. Before irradiation, the suspension containing the target contaminant and photocatalysts were sonicated for 3 min, and then continuously stirred in dark for 40 min in order to reach an adsorption-desorption equilibrium. After different irradiation intervals, each sample for analysis was taken from the reaction suspension with after-treatment of centrifugation at 5000 rpm for 20 min to remove the photocatalyst powders. The clarified solution was analyzed by UV-2700 UV-vis spectrometer (Shimadzu, Japan) to obtain the absorbance of the target contaminant at their maximum absorption wavelength. The degradation rate (D) of MB could be calculated by D = (1- C_t / C_0) × 100%, where C_0 and C_t are the equilibrium concentration

of the target contaminant before and after visible-light irradiation, respectively. After a complete cycle, the reborn CoPc/TiO_2 catalyst was tested in the fresh solution of MB under the same experimental conditions as mentioned above.

3. Results and discussion

3.1. SEM and TEM images

The SEM and TEM images of bare TiO_2 (a, c) and the CoPc/TiO_2 nanocomposites (b, d) with the molecular formula of TiO_2 (e) and CoPc (f) are displayed in Fig. 1. It can be seen clearly from Fig. 1a and 1b that bare TiO_2 nanoparticles show slight agglomeration with a regular shape around 0.1 μm microspheres while the particle profile of CoPc/TiO_2 came out to be more blurred. After dye sensitization, obvious agglomeration can be seen due to some of particles in the composite become more tightly associated than bare TiO_2 which ascribed to the successful sensitization from the CoPc dye to the TiO_2 surface and closer connections were constructed. The TEM images of bare TiO_2 (Fig. 1c) and the CoPc/TiO_2 nanocomposites (Fig. 1d) represent visual impression and further reveal that bare TiO_2 particles exhibit clear particle profile and slight agglomeration with an irregular shape which own a size around 30 nm, while after being sensitized by CoPc, the basic morphology of the composite was still retained, moreover particle profile become roughened and obvious agglomeration can be seen in Fig. 1d which is almost in agreement with the SEM result.

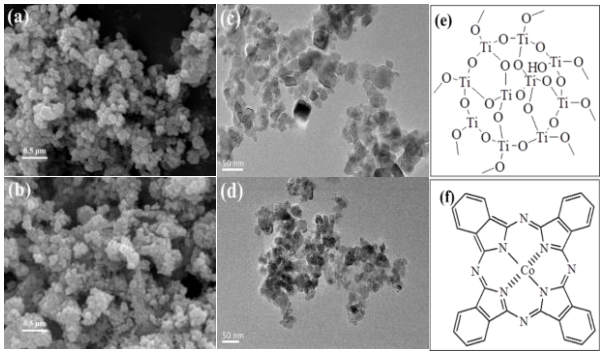

Fig. 1. SEM and TEM images of bare TiO_2 (a, c) and CoPc/TiO_2 nanocomposites (b, d) with the molecular formula of TiO_2 (e) and CoPc (f).

3.2. XRD patterns

The XRD patterns of CoPc dye and CoPc/TiO_2 with different mass ratio from 1:1 to 1:4 and bare TiO_2 nanoparticles are illustrated in Fig. 2. The characteristic diffraction peaks of bare TiO_2 at 2θ = 25.3, 37.8, 48.0 and 54.3° can be assigned to (101), (004), (200) and (105) crystal plane of anatase TiO_2 (JCPDS Card No. 01-0562), while diffraction peaks at 27.4, 36.0, 41.2, 55.2 and 56.6° can be assigned to (110), (101), (111), (211) and (220) crystal plane of rutile TiO_2 (JCPDS Card No.75-1757). Extra obvious diffraction peaks at 2θ from 10 to 20° can be found in the curves of the CoPc/TiO_2 nanocomposites reveal the existence of CoPc (ε-type) [12] which ascribed to its characteristic diffraction peaks compared with bare TiO_2, indicating that the CoPc molecules have been well sensitized with TiO_2 nanoparticles. Furthermore, the reflection peaks are becoming sharper with dye amount increase, and among which the mass ratio of 1:3 holds the optimal peak intensity with best sensitization synergistic effect. The average crystalline sizes of bare TiO_2 and the CoPc/TiO_2 (1:3) nanocomposites were figured out from the Debye-Scherrer formula to be approximately 18.6 nm and 23.1 nm, respectively, in good agreement with the TEM observation, and small-sized crystals are also beneficial for the separation of photogenerated hole and electron pairs because of quantum-size effects [23].

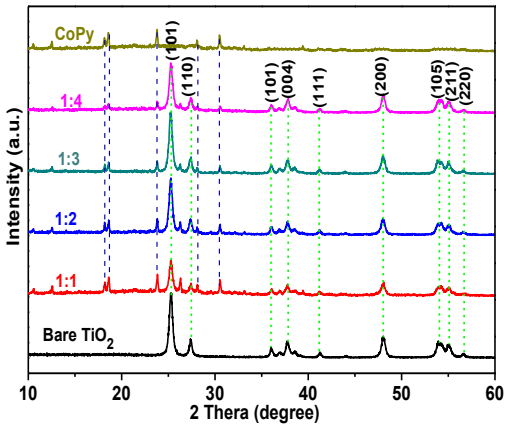

Fig. 2. XRD patterns of bare TiO_2 and CoPy and CoPc/TiO_2 nanocomposites (1:1-4).

3.3. FT-IR analysis

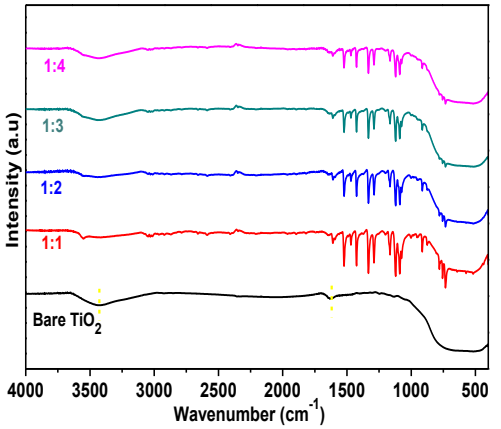

Fig. 3. FT-IR spectrum of bare TiO_2 and CoPc/TiO_2 nanocomposites (1:1-4).

The FT-IR spectra of bare TiO_2 and CoPc/TiO_2 nanocomposites with different mass radio (1:1-4) are shown in Fig. 3. A wide absorption band at 400-800 cm^{-1} corresponds to the stretching vibration of Ti-O band, and the absorption bands at 1628 and 3410 cm^{-1} represent the vibration of adsorbed water [24] in FT-IR analysis. After sensitized by CoPc dye, CoPc/TiO_2 nanocomposites retain the characteristic diffraction peaks of bare TiO_2, and the trend of four curves restrain the same. Meanwhile, the main characteristic absorption bands at 800-1700 cm^{-1} which attributed to the function groups of CoPc dye and the characteristic peaks of TiO_2 are kept, indicating that the CoPc molecules have well adsorbed to the TiO_2 surface.

3.4. UV-vis diffuse reflectance spectra

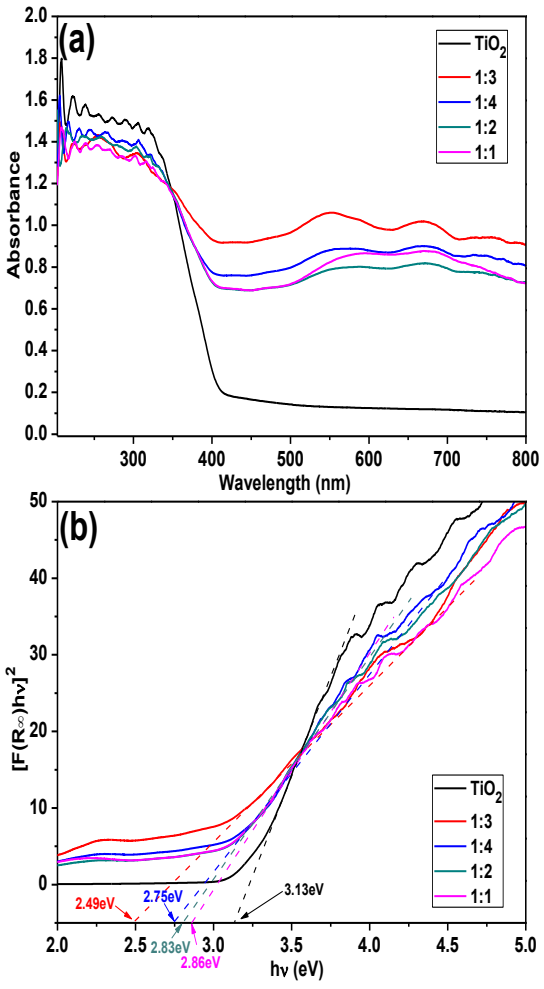

Fig. 4. UV-vis diffuse reflectance spectra (a) and calculated optical band gap (b) of bare TiO_2 and CoPc/TiO_2 composites (1:1-4).

The UV-vis diffuse reflectance spectra and optical band gap calculated via Tauc plot equation [25] of TiO_2 and the CoPc/TiO_2 nanocomposites (1:1-4) are shown in Fig. 4a and 4b. Bare TiO_2 only exhibit the fundamental absorption band of the UV region. The absorption region of the CoPc/TiO_2 nanocomposites is remarkably extended to visible-light region which demonstrate the TiO_2 particles sensitized via CoPc dye possess tremendous visible-light harvesting capacity. Plots of log(αhv) versus log(hv) are employed to obtain the exponent n, which corresponds to the slope of the tangent [26], and the slope of the tangent of CoPc/TiO_2 turns out to be 2, which corresponds to direct band gap transitions for CoPc sensitized TiO_2. The band gap of different samples are given in Fig. 4b as following sequence: Bare TiO_2 (3.13 eV) > CoPc/TiO_2 (1:1) (2.86 eV) > CoPc/TiO_2 (1:2) (2.83 eV) > CoPc/TiO_2 (1:4) (2.75eV) > CoPc/TiO_2 (1:3) (2.49 eV) which possess enhanced photocatalytic activity around 500 nm calculated via the equation of $E_g = 1240 / \lambda$.

3.5. Photocatalytic activities of CoPc dye sensitized TiO_2 nanoparticles

Fig. 5a show the temporal changes in absorption spectra of MB solution (25 mg/L) in the present of bare TiO_2 and CoPc/TiO_2 (take mass ratio of 1:3 as example) nanocomposites under visible-light irradiation. No other spectral features are evident in the absorption spectra after visible-light irradiation, indicating that the depletion of MB concentration in the solution is due to a thorough photochemical composition.

The photocatalytic activities of different CoPc/TiO_2 nanocomposites under simulative visible light irradiation are shown in Fig. 5b. Fig. 5b illuminates the degradation rate of the MB (25 mg/L, 50 mL) in the presence of 10 mg of the nanocomposites under visible-light irradiation. We can see clearly that CoPc/TiO_2 (1:3) exhibited much higher degradation rate than the other photocatalysts which owned approximately 98% degradation rate after 270 min visible-light irradiation. The kinetic data for the degradation process in the presence of CoPc/TiO_2 nanocomposites under visible light irradiation is demonstrated in Fig. 5c. It was found that the degradation reaction for all nanocomposites followed the Langmuir-Hinshewood (L-H) apparent first-order reaction model $\ln (C_0/C_t) = k_{app}t$ where C_0 is the concentration of pollutant after darkness absorption for 40 min, C_t is the concentration of MB at instant time t, and k_{app} is the apparent rate constant (min^{-1}). The apparent rate constants are determined for all tested photocatalysts form the slop of the line.

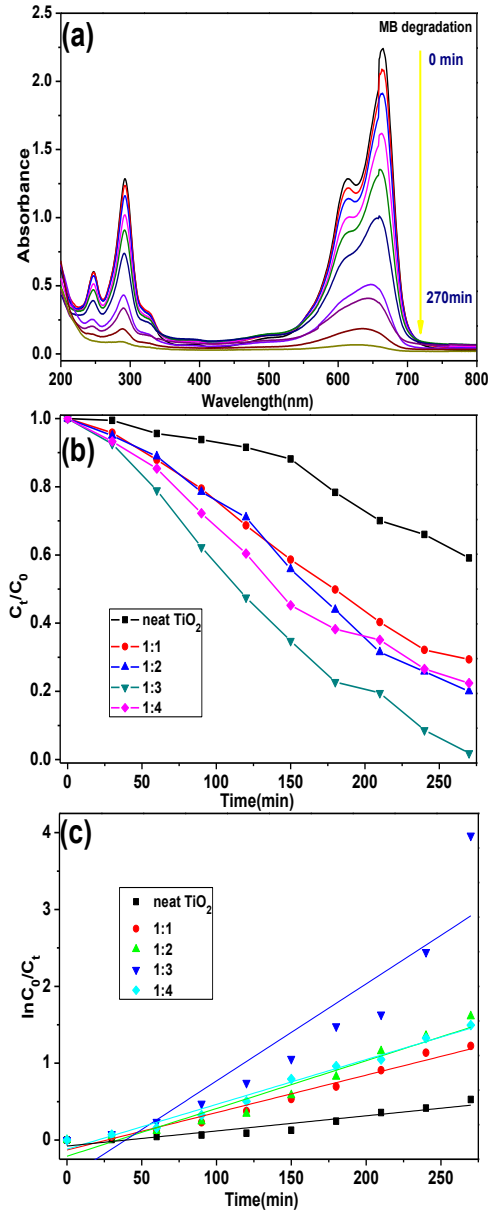

Fig. 5. Temporal changes in absorption spectra (a), the photocatalytic activities (b) and the kinetic data (c) of MB solution in the present of neat TiO_2 and CoPc/TiO_2 nanocomposites under visible-light irradiation.

The obtained apparent rate constant, linear regression coefficient (R^2) and degradation rate of MB are summarized in Table 1. We can see that the highest k_{app} value of the CoPc/TiO_2 (1:3) photocatalyst in MB degradation is 0.0126 min^{-1}, which is approximately 6.6 times larger than that of bare TiO_2 (0.0019 min^{-1}). The above results indicated that the CoPc sensitization made contribution to the degradation of MB with the CoPc/TiO_2 nanoparticle photocatalysts, and could obviously enhance the photocatalytic activity of TiO_2 under visible light. What's more, CoPc/TiO_2 composites (1:3) exhibit excellent photocatalytic activity than the others which was in accordance with the results of the calculated band gap.

Table 1. Apparent rate constant of MB photodegradation along with their linear regression coefficients of CoPc/TiO_2 nanocomposites (1:1-4).

	Decontamination of MB		
	k_{app}/ $(min)^{-1}$	R^2	Degradation rate after irradiating 270 min (%)
Bare TiO_2	0.0019	0.97	40.91
CoPc/TiO_2(1:1)	0.0048	0.941	70.63
CoPc/TiO_2(1:2)	0.0062	0.84	79.99
CoPc/TiO_2(1:3)	0.0126	0.982	98.10
CoPc/TiO_2(1:4)	0.0058	0.899	77.56

3.6. Photostability of the photocatalysts and TOC analysis

The photocatalytic stability of CoPc/TiO_2 nanocomposites was performed with 10 mg of the catalyst dosage in regulation irradiation time for each cycling run in MB solution (25 mg/L). The regeneration of photocatalyst was done by filtering the suspension to remove the bulk solution, and drying at 60 ^oC. The recovered CoPc/TiO_2 nanocomposites were reused in the next cycle. The result displayed in Fig. 7a shows that after 5 successive cycles under the visible-light irradiation, the degradation rate of MB is still up to 74% which declined from 98%, indicating that CoPc/TiO_2 nanocomposites possess excellent photocatalytic stability. Meanwhile the results above demonstrate a feasibility of recovery and reuse of CoPc/TiO_2 nanocomposites.

In order to verify the degradation of MB deeply, TOC test (b) was employed. MB can fade in color due to the breakage of only one double bond, so the TOC (Total Organic Carbon) test becomes the best method to stand for the degradation activity. This analysis was carried out using a total organic carbon (TOC) analyzer (Shimadzu TOC-VCHV) equipped with a platinum catalyst. The TOC test result is given below in Fig. 7b. The TOC value of pure MB solution turns out to be 8.5281 mg/L, however, the TOC value of MB solution improved with the increase of illumination time such as 9.9048 mg/L (60 min illuminated via visible-light marked as S1) and 19.351 mg/L (150 min illuminated via visible-light marked as S2). MB was proposed to degrade and mineralize to some complicated organic molecule [27] with larger molecule weight. Finally, with the end of the decomposition process, MB molecular was degraded thoroughly with a fairly small TOC value of 0.7076 mg/L (marked as S3). The specific data of TOC values of MB solution irradiated at

different reaction times and their corresponding integration area are incorporated in Table 2.

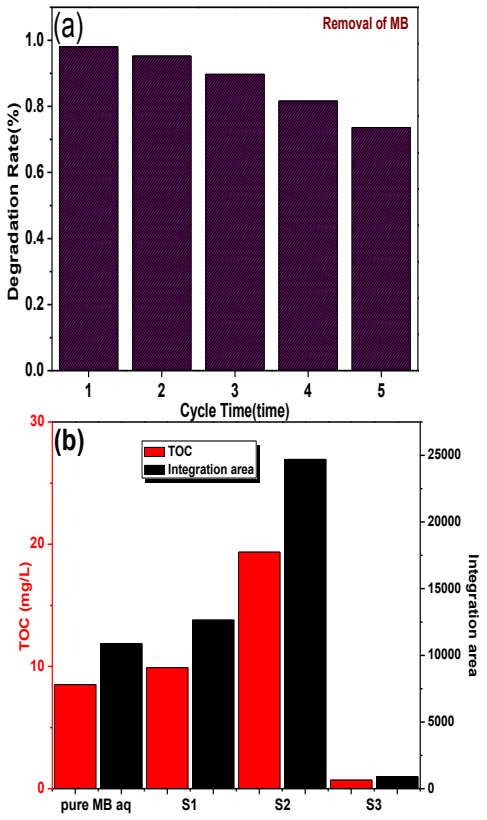

Fig. 7. Photocatalytic degradation rate of MB for CoPc/TiO_2 nanocomposites at different cycling time (a) and TOC analysis (b).

Table 2. TOC Values of MB Solution Irradiated at Different Reaction Times and Their Corresponding Integration Area.

	Pure MB aq	S1	S2	S3
TOC concentration / (mg/L)	8.5281	9.9048	19.351	0.7076
Integration area	10869.5	12639	24693	903

3.7. Possible connection action between CoPc dye and TiO_2

The detailed structure of CoPc on TiO_2 nanoparticles was proposed, and the possible interaction between CoPc and TiO_2 is illustrated in Fig. 8. The valid connection sites, both the nitrogen element from CoPc and the oxygen element from the framework TiO_2 possess excess unshared pair electrons provide the possibility of bonding, which represents a stronger acting force than simple physical adsorption. Planar structure of the CoPy dye is easier to connect with TiO_2 surface. Appropriate utilization of space provides a more comfortable spatial distance for both TiO_2 and CoPc dye. According to the study of Miguel et al.[28], the type and length of the functional group of a dye that is attached to the TiO_2 surface take a toll on the catalytic efficiency, which can be observed from the results for the photodegradation rates of MB. Under irradiation, the combination of the CoPc dye on the surface of TiO_2 nanoparticles improves photogenerated electron-hole pair separation and facilitates photogenerated charge transfer between the efficient charge transport of CoPc dye and TiO_2 framework to reduce the recombination rate of excited carreers [29]. Understanding these charge transfer process and designing the connection configuration at the molecular level are essential for further improvement. The excellent photocatalytic activity exhibited by CoPc/TiO_2 composite can ascribed to the existence of potential bonding interaction, as the flat structure of the dye molecular provides favorable edges of space.

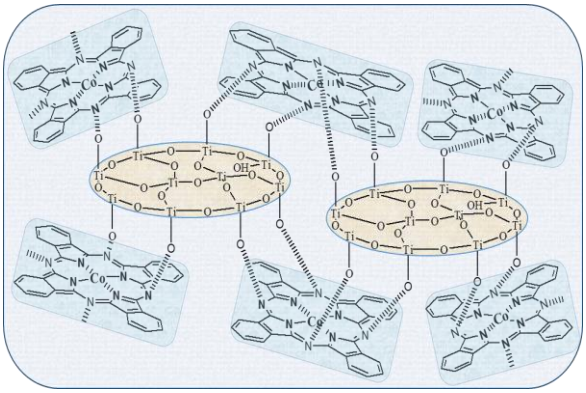

Fig. 8. Detailed structure of CoPc on TiO_2 nanoparticles and the possible interaction between CoPc and TiO_2.

3.8. Visible light induced photocatalytic mechanism

Fig. 9 shows the visible-light induced photocatalytic mechanism of CoPc/TiO_2 nanoparticles. As is known to all, electron-hole pairs (e^--h^+) are formed when the photons have energy which matches or exceeds the band gap energy of TiO_2 (3.2 eV). In the present study, the sensitization of CoPc dye to TiO_2 surface could be easily excited by from the ground state (Dye) to the excited state (Dye^*) of dye by the action of a visible light photon. It is known that the higher separation efficiency of electron-hole pairs will enhance photocatalytic activity and results in a large number of holes participated in the photocatalytic process [30]. Stability is sustained by keeping excited electrons away from TiO_2, i.e., the photo-induced electrons are transferred rapidly and

injected into CoPc from the conducting band of TiO_2, thereby avoiding recombination of h^+ and e^- during the photocatalytic process [31]. Various oxidation-reduction reactions were taken place on the TiO_2 surface, the MB molecules were easy to degrade and mineralize to the degradation product such as CO_2 and H_2O via a series of protonation and reduction steps [32]. In a word, CoPc/TiO_2 nanocomposites play an important role for better environmental management under visible-light illumination.

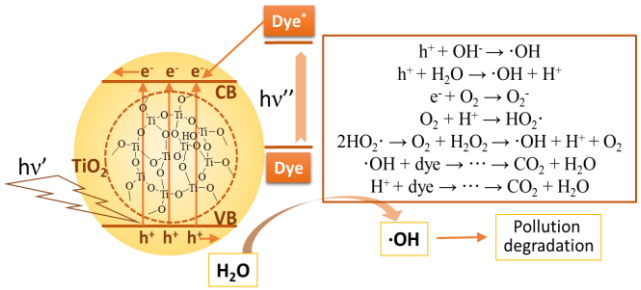

Fig. 9. Dye-sensitized and band gap absorption-initiated paths of MB degradation.

4. Conclusion

Complete nanocomposites fabricated with TiO_2 particles, sensitized with cobalt phthalocyanine dye by ultrasonic immersing-hydrothermal sensitization method, have been studied by using a variety of characterization methods. After CoPc sensitization, the photoresponse range of TiO_2 extended to visible-light region is of great importance for the enhanced photocatalytic activity which holds tremendous light harvesting capacity and possess enhanced photocatalytic efficiency. Moreover, their optical band gap calculated via Tauc plot equation deduced accordingly and specific wavelength of visible-light (absorption spectra of CoPc/TiO_2 1:3 mass ratio turns out to be around 500 nm) was calculated by using $E=1240/\lambda$. Great photostability of nanocomposites can be achieved from the recycling experiment. Among the different mass ratio of the nanocomposites, CoPc/TiO_2 (1:3) achieve the optimal photocatalytic degradation rate and mineralization effect of MB degradation under visible-light irradiation, showing great potential in detoxification of harmful pollutants in wastewaters. Excellent CoPc/TiO_2 nanocomposite catalysts will become a promising candidate in the field of protection of resources, environmental protection and ecological conservation.

Acknowledgements

This work was financially supported by Research Foundation for the Practice and Innovation Training Project for College Students of Jiangsu Province (NO. 201312920001Y), the Research Project of Nanjing College of Chemical Technology (NHKY-2013-3) and Scientific Program of QiMing Project (NHKY-QMGC-2015-07).

References

[1] J. Jiang, F. Gu, W. Shao, C. Li, Ind. Eng. Chem. Res. **51**, 2838 (2012).
[2] K. Hashimoto, H. Irie, A. Fujishima, J. Appl. Phys. **44**, 8269 (2005).
[3] F. Chen, W. Zou, W. Qu, J. Zhang, Catal. Comm. **10**, 1510 (2009).
[4] A. E. Carina, I. L. Marta, K. Marinus, B. Michel, C. J. Christophe, Langmuir **22**, 3606 (2006).
[5] M. Dozzi, A. Saccomanni, E. Selli, J. Hazard. Mater. **211-212**, 188 (2012).
[6] Y. F. Li, W. P. Zhang, X. R. Li, Y. Yu, J. Phys. Chem. Solids **75**, 86 (2014).
[7] A. S. Mohamed, S. I. M. Mohamad, Y. A. A. Magdy, J. Alloys Comp. **509**, 2582 (2011).
[8] Q. Cheng, Y. Cao, L. Yang, P. Zhang, K. Wang, H. Wang, Mater. Res. Bull. **46**, 372 (2011).
[9] L. Yang, W. Sun, S. Luo, Y. Luo, Appl. Catal. B: Environ. **156-157**, 25 (2014).
[10] S. An, B. Joshi, M. Lee, N. Kim, S. Yoon, Appl. Surf. Sci. **294**, 24 (2014).
[11] G. Qin, Z. Sun, Q. Wu, L. Lin, M. Liang, S. Xue, J. Hazard. Mater. **192**, 599 (2011).
[12] J. F. Shen, N, Li, M. X. Ye, J. Alloys Comp. **580**, 239 (2013).
[13] O. Akhavan, ACS Nano **4**, 4174 (2010).
[14] E. Toshio, H. Ryo, Chem. Mater. **3**, 918 (1991).
[15] M. E. Sánchez-Vergaraa, M. Rivera, J. Phys. Chem. Solids **75**, 599 (2014).
[16] M. Giuseppe, G. L. Elisa, P. Leonardo, D. Gabriela, S. Rudolf, J. Phys. Chem. C **111**, 6581 (2007).
[17] J. F. Myers, G. W. R. Canham, A. B. P. Lever, Inorg. Chem. **14**, 461 (1975).
[18] R. F. Parton, I. F. J. Vankelecom, M. J. A. Casselman, C. P. Bezoukhanova, J. B. Uytterhoeven, P. A. Jacobs, Nature **370**, 541 (1994).
[19] M. K. Halbert, R. P. Baldwin. Anal. Chem. **57**, 591 (1985).
[20] P. Giovanni, C. G. Marı´a, L. F. Marı´a, D. G. L. Marı´a, A. Vincenzo, Y. Sedat, P. Mario, J. Phys. Chem. C **112**, 2667 (2008).
[21] I. Nobuyuki, F. Daisuke, J. Phys. Chem. C **116**, 20300 (2012).
[22] G. Serpil, T. Ece, B. Zekeriya, K. Halit, Synthetic Met. **176**, 108 (2013).
[23] T. Peng, D. Zhao, K. Dai, W. Shi, K. Hirao, J. Phys. Chem. B **109**, 4947 (2005).
[24] T. Zhang, T. Oyama, A. Aoshima, H. Hidaka, J. Zhao, N. Serpone, J. Photochem. Photobiol. A Chem. **140**,

163 (2001).
[25] J. Tauc, Mat. Res. Bull. **3** (1968) 37-46.
[26] A. Nakajima, Y. Sugita, K. Kawamura, H. Tomita, N. Yokoyama, J. Appl. Phys. **80**, 4006 (1996).
[27] A. Houas, H. Lachheb, M. Ksibi, E. Elaloui, C. Guillard, J. M. Herrmann, Appl. Catal. B: Environ. **31**, 145(2001).
[28] G. D. Miguel, M. Marchena, B. Cohen, S. S. Pandey, S. Hayase, A. Douhal, J. Phys. Chem. C **116**, 22157 (2012).
[29] X. Bai, X. Y. Zhang, Z. L. Hua, W. Q. Ma, Z. Y. Dai, X. Huang, H. X. Gu, J. Alloys Comp. **599**, 10 (2014).
[30] K. Li, J. Xiong, T. Chen, L. Yan, Y. Dai, D. Song, Y. Lv, Z. Zeng, J. Hazard. Mater. **250-251**, 19 (2013).
[31] P. Theodora, P. X. Nikolaos, P. Ioannis, M. Dionissios, J. Photochem. Photobiol. A Chem. **186**, 308 (2007).
[32] K. L. Lv, X. F. Li, K. J. Deng, J. Sun, X. H. Li, M. Li, Appl. Catal. B: Environ. **95**, 83 (2010).

*Corresponding author: yuancai@njtech.edu.cn
wyt@njcc.edu.cn